RAR1, a central player in plant immunity, is targeted by *Pseudomonas syringae* effector AvrB

Yulei Shang*, Xinyan Li*†, Haitao Cui*, Ping He†, Roger Thilmony‡, Satya Chintamanani†, Julie Zwiesler-Vollick‡, Suresh Gopalan‡, Xiaoyan Tang†, and Jian-Min Zhou*§

*National Institute of Biological Sciences, Beijing 102206, China; †Department of Plant Pathology, Kansas State University, Manhattan, KS 66506; and ‡Department of Energy Plant Research Laboratory, Michigan State University, East Lansing, MI 48824

Edited by Brian J. Staskawicz, University of California, Berkeley, CA, and approved October 24, 2006 (received for review August 22, 2006)

Pathogenic bacterial effectors suppress pathogen-associated molecular pattern (PAMP)-triggered host immunity, thereby promoting parasitism. In the presence of cognate resistance genes, it is proposed that plants detect the virulence activity of bacterial effectors and trigger a defense response, referred to here as effector-triggered immunity (ETI). However, the link between effector virulence and ETI at the molecular level is unknown. Here, we show that the *Pseudomonas syringae* effector AvrB suppresses PAMP-triggered immunity (PTI) through RAR1, a cochaperone of HSP90 required for ETI. AvrB expressed in plants lacking the cognate resistance gene *RPM1* suppresses cell wall defense induced by the flagellar peptide flg22, a well known PAMP, and promotes the growth of nonpathogenic bacteria in a *RAR1*-dependent manner. *rar1* mutants display enhanced cell wall defense in response to flg22, indicating that RAR1 negatively regulates PTI. Furthermore, coimmunoprecipitation experiments indicated that RAR1 and AvrB interact in the plant. The results demonstrate that RAR1 molecularly links PTI, effector virulence, and ETI. The study supports that both pathogen virulence and plant disease resistance have evolved around PTI.

bacterial virulence | disease resistance | innate immunity | type III effector

Microbe-derived molecules such as bacterial flagellin and lipopolysaccharides, collectively called pathogen-associated molecular patterns (PAMPs) or microbe-associated molecular patterns (MAMPs; ref. 1), trigger immunity in both animals and plants. Similar to many Gram-negative bacterial pathogens, *Pseudomonas syringae* uses the type III secretion system to deliver effector proteins into host cells to promote parasitism (2). Emerging evidence indicates that many of the effectors function by actively suppressing PAMP-triggered immunity (PTI; refs. 3 and 4).

Some of the effectors are recognized by host surveillance systems and trigger a strong resistance when their cognate resistance genes are present (2, 4). Often, this so-called "gene-for-gene resistance" or effector-triggered immunity (ETI; ref. 4) is activated by an indirect interaction between the resistance protein and the cognate effector protein (5). Three proteins, HSP90, RAR1, and SGT1, play an important role in ETI by regulating the stability of NB-LRR resistance proteins (6–11), but they are not known for a role in PTI regulation. It is thought that the plant resistance gene products somehow sense the virulence activity of these effectors, rather than the effectors themselves, which in turn activates resistance. Supporting this hypothesis, several host proteins have been shown to interact with both effector and resistance proteins and are required for ETI (12–16). However, a role of these proteins in effector-mediated virulence function remains to be demonstrated.

The *P. syringae* effector protein AvrB enhances virulence on soybean and *Arabidopsis* plants lacking cognate resistance genes but triggers ETI on soybean and *Arabidopsis* plants carrying the resistance genes (17). The virulence function of AvrB is expressed as increased bacterial growth in soybean plants and leaf chlorosis in *Arabidopsis* plants. The virulence and ETI activity of AvrB have the same structural requirements, suggesting that the virulence function and ETI are intimately connected (17, 18). Therefore, host proteins required for AvrB virulence function may provide a molecular link between effector virulence function and ETI.

Here we show that AvrB inhibits PTI through RAR1, a HSP90 cochaperone required for disease resistance gene functions. When expressed in plants, AvrB suppresses plant defenses and enhances bacterial growth in a RAR1- and jasmonate (JA) pathway-dependent manner. Furthermore, *rar1* mutants exhibit an enhanced cell wall defense response to flg22, indicating that RAR1 is a negative regulator of basal defense and that RAR1 plays a central role in both PTI and ETI.

Results

RAR1 Is Required for the Induction of a JA-Response Gene by *P. syringae* (*avrB*). We have shown previously that the AvrB effector delivered by *P. syringae* bacteria induces *Arabidopsis RAP2.6* gene expression in the absence of the cognate resistance gene *RPM1* (19), although the presence of *RPM1* further enhances this induction (data not shown). The induction requires COI1, an F-box protein essential for JA signaling (20). To identify additional host factors required for AvrB function, we sought to screen for *Arabidopsis* mutants that failed to induce *RAP2.6* in response to AvrB. A *RAP2.6-LUC* reporter line (19) was mutagenized by ethane methyl sulfonate, and 16,000 M_2 plants derived from 9,000 M_2 families were screened by infiltrating *P. syringae* DC3000 (*avrB*) bacteria into leaves. Plants displaying reduced *RAP2.6-LUC* expression (reduced responsiveness to *avrB;rrb*) were selected and further confirmed in the M_3 generation. Seven *rrb* mutants were identified. One mutant, *rrb3*, displaying a loss of *avrB*-specific induction of *RAP2.6-LUC* was characterized in detail. Fig. 1*A* shows that *RAP2.6-LUC* reporter activity was strongly activated by DC3000 (*avrB*) in the wild-type transgenic line 6 h after inoculation. In contrast, luciferase (LUC) activity was reduced by 3-fold in the *rrb3* mutant, a level identical to plants treated with DC3000 lacking *avrB* (Fig. 1*B*), indicating that the *rrb3* mutant was rendered insensitive to *avrB*. RNA blot analysis showed that the endogenous *RAP2.6* transcript level following DC3000 (*avrB*) infiltration was similarly reduced in the *rrb3* mutant [supporting information (SI) *Supporting Text* and SI Fig. 7]. However, *RAP2.6-LUC* expression in response to DC3000 lacking *avrB* was not altered in *rrb3* (Fig.

Author contributions: Y.S., X.L., and H.C. contributed equally to this work; X.L. and J.-M.Z. designed research; Y.S., X.L., H.C., P.H., R.T., and S.C. performed research; R.T., J.Z.-V., S.G., and J.-M.Z. contributed new reagents/analytic tools; Y.S., X.L., X.T., and J.-M.Z. analyzed data; and X.T. and J.-M.Z. wrote the paper.

This article is a PNAS direct submission.

Abbreviations: PAMPs, pathogen-associated molecular patterns; JA, jasmonates, PTI, PAMP-triggered immunity; ETI, effector-triggered immunity; Dex, dexamethasone; LUC, luciferase.

§To whom correspondence should be addressed. E-mail: zhoujianmin@nibs.ac.cn.

This article contains supporting information online at www.pnas.org/cgi/content/full/0607279103/DC1.

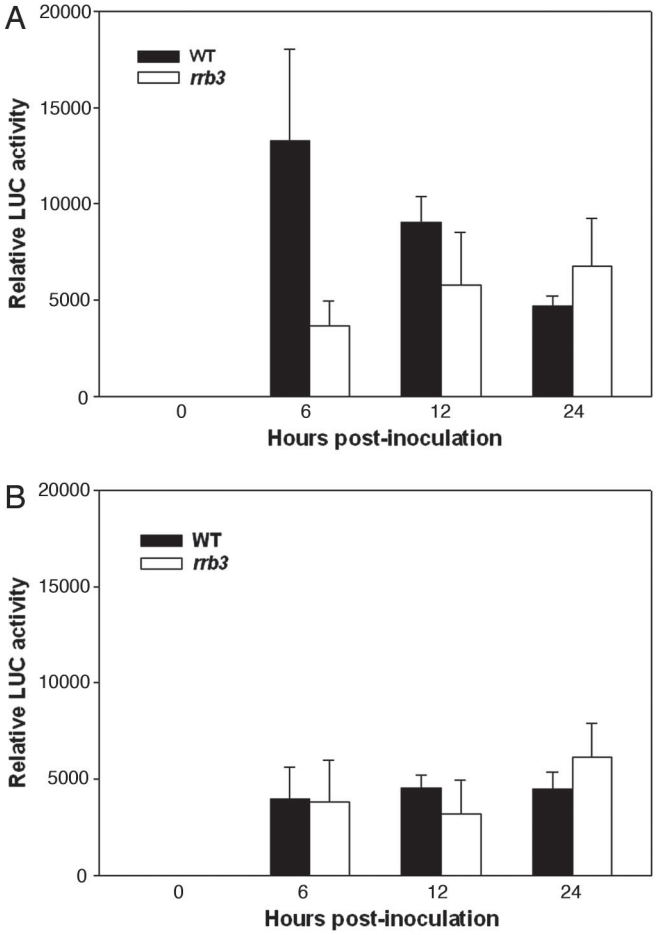

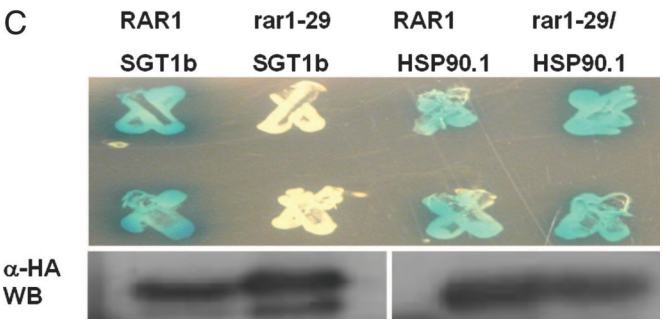

Fig. 1. *rrb3* does not respond to AvrB delivered by *P. syringae*. (*A* and *B*) *RAP2.6-LUC* reporter activity of WT transgenic plants and *rrb3* in response to DC3000 (*avrB*) (*A*) or DC3000 (*B*). The *RAP2.6-LUC* assay on *rrb3* was performed four times with similar results. (*C*) Yeast two-hybrid assay for rar1–29 interaction with SGT1b and HSP90. (*Upper*) X-Gal assay. At least six individual colonies from each transformation were tested for β-galactosidase activities on X-Gal plates, and two representative clones are shown. (*Lower*) Western blot for RAR1-HA and rar1–29-HA protein detected with an anti-HA monoclonal antibodies.

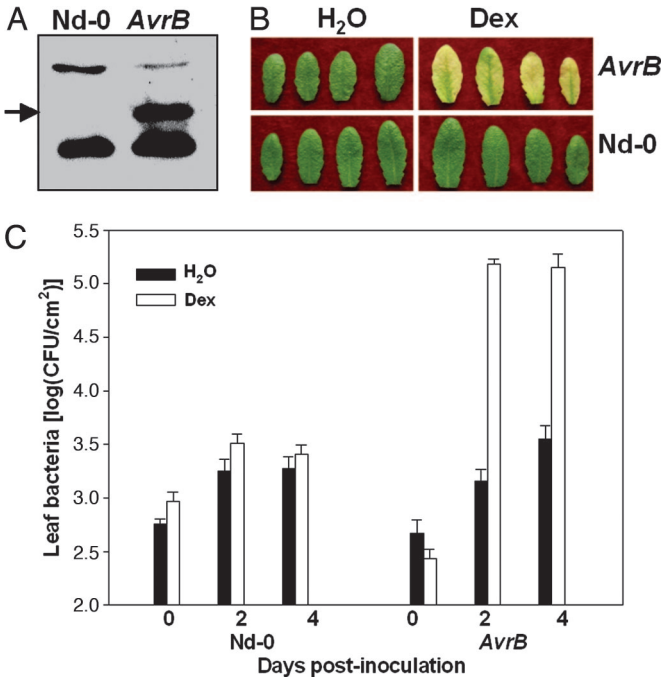

Fig. 2. Overexpression of AvrB induces chlorosis and enables nonpathogenic *P. syringae* mutant growth. (*A*) Induced accumulation of AvrB protein (arrow) after Dex treatment. Wild-type (Nd-0) and *AvrB* transgenic plants were sprayed with 30 μM Dex and harvested after 24 h for protein extraction. (*B*) Leaf chlorosis 4 days after daily spraying with 30 μM Dex or H_2O. All seven independent *AvrB* transgenic lines tested showed similar phenotypes. (*C*) DC3000 *hrpL* mutant bacterial population in wild-type (Nd-0) and *AvrB* transgenic plants treated with H_2O or Dex. The bacterial growth assay was repeated twice with similar results.

1*B*), indicating an AvrB-specific defect. Both the wild-type *RAP2.6-LUC* transgenic plants and *rrb3* contain *RPM1*, the cognate resistance gene for *avrB*. We therefore tested whether the *rrb3* mutation impacts the effector-triggered resistance. When inoculated with DC3000 (*avrB*) at a high dose, the *rrb3* mutant showed a delayed hypertensitive response (HR) (SI Supporting Text, Fig. 8 and SI Table 1). Bacterial growth assay indicated that the *rrb3* was completely susceptible to DC3000 (*avrB*) (SI Fig. 9). Genetic analysis indicated that *rrb3* the phenotype was caused by a single recessive mutation. The *rrb3* mutation was mapped to chromosome 5 between BACs K10D11 and MIO24, a 46-kb interval containing *RAR1* (data not shown). Complementation tests indicated that *rrb3* is a *rar1* allele, because *rrb3* × *rar1–20* F_1 plants displayed a delayed HR and reduced *RAP2.6-LUC* expression (SI Table 1) in response to DC3000 (*avrB*). Sequencing analysis indicated that the *rrb3* mutant carried a point mutation in *RAR1* that led to a H217Y substitution. Transformation of the wild-type *RAR1* gene into *rrb3* restored the normal HR induction (data not shown). The *rrb3* mutation reduced the level of RAR1 protein accumulation in plants (SI Fig. 10). Twenty-eight *rar1* alleles had been reported before this study (21); we therefore renamed *rrb3* as *rar1–29*. H217 is a highly conserved residue located in the CHORD II domain of the RAR1 family proteins. The CHORD II domain is known to be required for interaction with SGT1 but not HSP90 (6). Indeed, the yeast two-hybrid experiment indicated that the rar1–29 mutant was unable to interact with SGT1b but interacted normally with HSP90.1 (Fig. 1*C*).

Expression of *AvrB* in Plants Enhances Disease Susceptibility and Causes Chlorosis. When delivered by *P. syringae*, AvrB confers virulence on soybean plants lacking the cognate resistance gene *Rpg1* (22). A similar virulence function was not detected in *Arabidopsis* when delivered by *P. syringae* bacteria. However, when directly expressed in plants lacking the *RPM1* gene, AvrB induces leaf chlorosis that is reminiscent of disease symptoms, suggesting a role of AvrB in virulence (23, 24). We similarly introduced the *AvrB* transgene into Nd-0, an ecotype lacking the cognate resistance gene *RPM1*, by using the dexamethasone (Dex)-inducible system (25). Fig. 2*A* shows that Dex treatment induces AvrB protein accumulation in the plant. Four days after

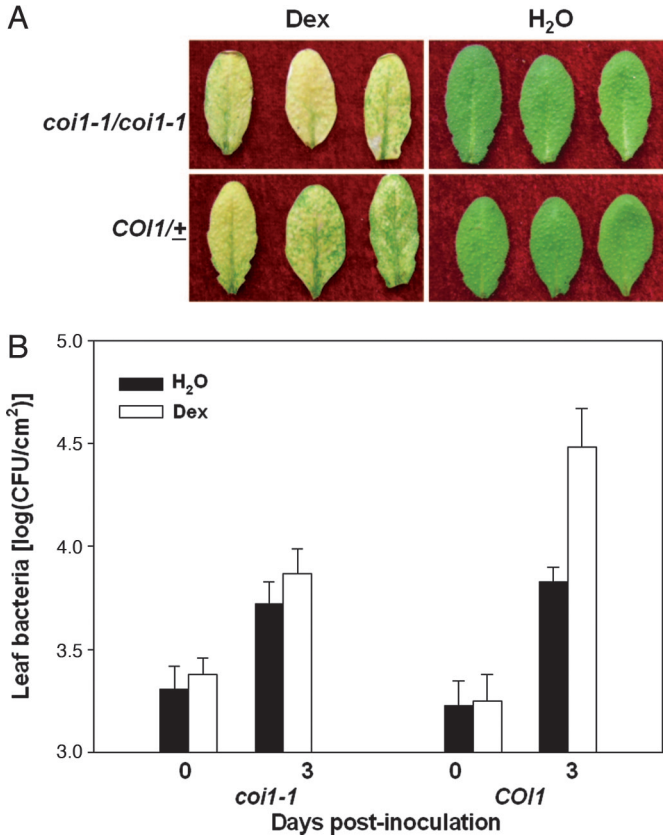

Fig. 3. *COI1* is required for AvrB-mediated bacterial growth. (*A*) AvrB-induced chlorosis. Photographs were taken 4 days after spray of Dex or H_2O. (*B*) DC3000 *hrpL* mutant bacterial growth in *COI1/COI1,rpm1/rpm1,AvrB/*± (*COI1*) and *coi1–1/coi1–1,rpm1/rpm1,AvrB/*± (*coi1*) plants pretreated with H_2O or Dex. Two independent experiments were done with similar results.

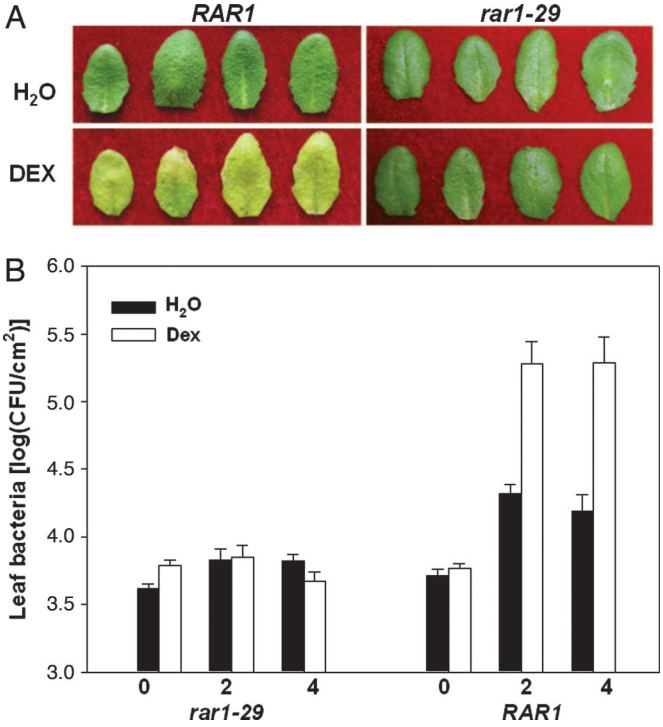

Fig. 4. *RAR1* is required for AvrB-induced leaf chlorosis and disease susceptibility. (*A*) AvrB-induced chlorosis. Photographs were taken 4 days after Dex or H_2O treatment. (*B*) DC3000 *hrpL* mutant bacterial growth in *RAR1/RAR1,rpm1/rpm1,AvrB/AvrB* (*RAR1*) and *rar1–29/rar1–29,rpm1/rpm1,AvrB/AvrB* (*rar1–29*) plants pretreated with H_2O or Dex. The experiments were repeated four times with similar results.

Dex treatment, AvrB-expressing leaves developed chlorosis, whereas the nontransgenic wild-type plants showed no symptoms (Fig. 2*B*). All seven independent transgenic lines displayed identical phenotype (data not shown). We further tested whether the chlorosis phenotype is associated with enhanced susceptibility by examining bacterial growth of a nonpathogenic strain lacking the *hrpL* gene that is required for the expression of type III genes and coronatine biosynthetic genes in the bacterium (26). Plants expressing AvrB enhanced the growth of the DC3000 *hrpL* mutant bacteria by up to 50-fold (Fig. 2*C*). These results support that AvrB can act as virulence factor to promote bacterial colonization in plants lacking *RPM1*.

The AvrB-Dependent Susceptibility Is COI1-Dependent. To determine whether the enhanced susceptibility phenotype caused by AvrB overexpression is relevant to the activity of AvrB delivered by *P. syringae*, we tested whether they require the same genetic components in plants. Because COI1 is required for *P. syringae* (*avrB*)-induced *RAP2.6* expression (19), we crossed the AvrB-expressing plants with the *coi1–1* mutant to construct F_2 plants with *COI1/COI1,rpm1/rpm1,AvrB/*± and *coi1–1/coi1–1,rpm1/rpm1,AvrB/*± genotypes. Treatment of these plants with Dex induced chlorosis in both genotypes (Fig. 3*A*), indicating that the chlorosis was independent of COI1. The Dex-treated plants were also inoculated with the DC3000 *hrpL* mutant bacteria. Fig. 3*B* shows that bacterial growth was enhanced in Dex-treated *COI1/COI1,rpm1/rpm1,AvrB/*± plants but not *coi1–1/coi1–1,rpm1/rpm1,AvrB/*± plants, suggesting that AvrB enhances bacterial growth by activating of the JA pathway. These results indicate that the AvrB virulence function is mediated, at least in part, by the JA signaling pathway.

RAR1 Is Required for AvrB-Dependent Susceptibility and Chlorosis. Because the *rar1–29* mutant was isolated from plants carrying *RPM1*, and RAR1 is required for RPM1 stability, the observed phenotype could result from reduced RPM1 protein in the *rar1–29* mutant. We therefore sought to determine whether *RAR1* is required for AvrB-enhanced susceptibility in plants lacking *RPM1* by crossing *rar1–29* to the AvrB-transgenic plants. Homozygous F_4 lines of *RAR1/RAR1,rpm1/rpm1,AvrB/AvrB* and *rar1–29/rar1–29,rpm1/rpm1,AvrB/AvrB* were generated and tested for chlorosis and enhanced susceptibility phenotypes associated with AvrB expression. As shown in Fig. 4*A*, Dex-induced chlorosis was observed in the *RAR1/RAR1,rpm1/rpm1,AvrB/AvrB* genotype but not the *rar1–29/rar1–29,rpm1/rpm1,AvrB/AvrB* genotype. Similarly, AvrB expression promoted DC3000 *hrpL* mutant bacterial growth only in *RAR1* plants but not in *rar1–29* plants (Fig. 4*B*).

Because *rar1–29* does not eliminate RAR1 protein accumulation, we also tested whether *rar1–20*, which lacks the entire *RAR1* locus (21), abolished virulence activity associated with *AvrB* expression. *rar1–20* was crossed to the *AvrB* transgenic plants to construct *rar1–20/rar1–20,rpm1/rpm1,AvrB/*± plants. As shown in SI Fig. 11, *rar1–20* completely abolished the ability of AvrB to enhance *hrpL* mutant bacterial growth in plants. Together, these results demonstrate that RAR1 is required for the virulence function induced by AvrB overexpression.

AvrB Suppresses PAMP-Induced Cell Wall Defense Through RAR1. Suppression of PTI is critical for bacterial virulence (3, 4). More than a dozen *P. syringae* effectors have been shown to suppress PAMP-induced defenses (27–30). Treatment of plants with the

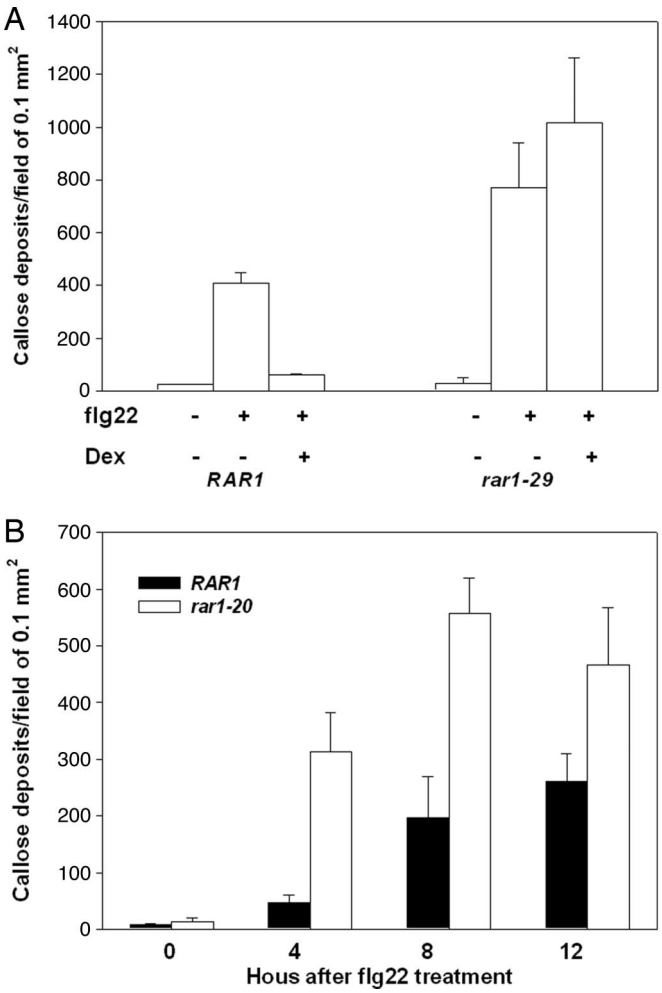

Fig. 5. *RAR1* negatively regulates flg22-induced callose deposition. (*A*) *RAR1* is required for AvrB-mediated suppression of callose deposition. Leaves from *RAR1/RAR1,rpm1/rpm1,AvrB/AvrB* (*RAR1*) and *rar1–29/rar1–29,rpm1/rpm1,AvrB/AvrB* (*rar1–29*) plants were sprayed with Dex or H_2O for 24 h before being induced with 50 μM flg22 for 12 h. Callose deposition was examined 12 h later. (*B*) *RAR1* attenuates flg22-induced callose deposition. *RAR1* and *rar1–20* plants were treated with 2 μM flg22 for the indicated hours before staining for callose. The number of callose deposits represents an average of four microscopic fields of 0.1 mm^2 obtained from four different leaves. Error bars represent standard error. Experiments were repeated four times with similar results.

flg22 peptide, a well known PAMP derived from bacterial flagellin, induces callose deposition, a cell-wall-based defense required for resistance to *Pseudomonas* bacteria (29, 31). We therefore tested whether AvrB overexpression suppressed the flg22-induced callose deposition. Indeed, although *RAR1/RAR1,rpm1/rpm1,AvrB/AvrB* plants treated with flg22 developed numerous callose deposits, a prespray of Dex reduced the flg22-induced callose deposition by ≈80% (Fig. 5*A*). In contrast, Dex treatment had no effect on callose deposition in the *rar1–29/rar1–29,rpm1/rpm1,AvrB/AvrB* genotype, indicating that *RAR1* is required for the suppression of flg22-induced callose deposition by AvrB.

RAR1 Is a Negative Regulator of PAMP-Induced Basal Defense. Interestingly, we reproducibly observed less callose deposition in *RAR1/RAR1,rpm1/rpm1,AvrB/AvrB* plants compared with *rar1–29/rar1–29,rpm1/rpm1,AvrB/AvrB* in the absence of Dex treatment (Fig. 5*A*), suggesting a negative role of *RAR1* in flg22-induced basal defense in the absence of effectors. To further test this possibility, we compared *rar1–20* and wild-type Col-0 plants, neither plant carries the *AvrB* transgene, for flg22-induced callose deposition. As shown in Fig. 5*B*, the wild-type plants reproducibly showed fewer callose deposits than did *rar1–20* plants. The effect of the *rar1–20* mutation was most prominent when plants were induced with a low concentration of flg22 (2 μM) and examined at early hours after flg22 treatment. Together, these results indicate that *RAR1* negatively regulates flg22-induced callose deposition.

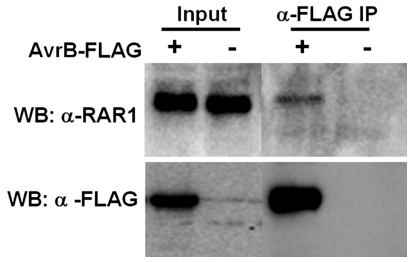

Fig. 6. RAR1 and AvrB interact in plants. Nontransgenic *rpm1* plants (−) and AvrB-3xFLAG transgenic *rpm1* plants (+) were sprayed with estradiol to induce protein expression. Coimmunoprecipitation was carried out with an anti-FLAG monoclonal antibody. The immunocomplex was subjected to Western blot analyses by using anti-RAR1 and -FLAG antibodies.

RAR1 and AvrB Are in the Same Complex. Yeast two-hybrid assays failed to detect an interaction between AvrB and RAR1 (data not shown). To determine whether AvrB is capable of interacting with RAR1 *in vivo*, we generated additional transgenic lines carrying AvrB-3xFLAG under the control of an estrogen-inducible promoter in the *rpm1* background (32, 33). Estradiol-induced expression of AvrB-3xFLAG resulted in typical leaf chlorosis (data not shown). Fig. 6 shows that RAR1 and AvrB-3xFLAG were coprecipitated by an anti-FLAG monoclonal antibody in extracts from AvrB-3xFLAG transgenic but not nontransgenic plants. This result indicates that AvrB and RAR1 are present in the same protein complex.

Because AvrB is known to interact with RIN4 (12), we asked whether RAR1 and RIN4 are in the same protein complex. A HA-tagged RIN4 was overexpressed in protoplasts (in the *rpm1* mutant background). Coimmunoprecipitation failed to detect RAR1 in the HA-RIN4 immunocomplex even when RAR1 was overexpressed, whereas AvrB-FLAG was successfully detected in the HA-RIN4 complex when coexpressed (SI *Supporting Text* Fig. 12), suggesting that RIN4 and RAR1 exist in different protein complexes.

Discussion

RAR1, together with SGT1 and HSP90, is known to play a key role in ETI to diverse pathogens (6–8, 21, 34–39). A role of these proteins in bacterial effector virulence function has not been reported. Our results show that RAR1 negatively regulates basal defense and is required for AvrB-mediated suppression of basal defense, providing a molecular link between the effector-mediated suppression of basal defense and *R* gene-mediated disease resistance.

RAR1 is known to act as a cochaperone of HSP90 to stabilize certain NB-LRR resistance proteins, including RPM1, the cognate resistance protein of AvrB (7–11, 21). Perhaps RAR1 also assists the accumulation of proteins that negatively regulate PAMP-induced defenses. Because *RAR1* is required for all aspects of AvrB-induced phenotypes, whereas *COI1* is required only for the enhanced bacterial growth in the plant, it is most likely that RAR1 acts upstream of COI1. It is not clear how RAR1 mediates the activation of JA signaling after AvrB

expression. One scenario is that RAR1 does so through the interaction with SGT1. Consistent with this speculation, rar1–29 is unable to interact with SGT1b. Although we have not tested whether it is required for AvrB virulence, SGT1b is known to play a role in JA signaling (40).

Although enhanced bacterial growth is observed only when AvrB is expressed in plants, two lines of evidence indicate that our findings are relevant to the AvrB function in the natural setting. Both the *P. syringae* (*avrB*)-induced *RAP2.6* gene expression and the AvrB-mediated bacterial growth required *COI1* (Fig. 3*B*; ref. 3). Similarly, RAR1 is required for both *P. syringae* (*avrB*)-induced *RAP2.6* gene expression and the *AvrB* transgene-dependent susceptibility and defense suppression (Figs. 1*A* and 4). These results support that the *AvrB* transgene-dependent susceptibility is intrinsically linked to the virulence function of the *P. syringae*-delivered AvrB.

The previously identified effector target proteins are required for ETI (13–16) but not the effector virulence function. For example, the RPM1-interacting protein RIN4 is an intensively studied effector target that mediates both RPM1 and RPS2 resistance by interacting with their cognate effectors AvrRpm1, AvrB and AvrRpt2. Similar to RAR1, the RIN4 protein also acts as a negative regulator that attenuates PAMP-induced callose deposition in the absence of the effectors (29). Both AvrRpm1 and AvrRpt2 were shown to suppress PTI. AvrRpt2 is a cysteine protease that cleaves RIN4 (13, 14, 16), whereas AvrRpm1 and AvrB cause the phosphorylation of RIN4 through an unknown mechanism (12). However, it remains unexplained why the degradation of RIN4 by AvrRpt2 does not enhance PTI in plants lacking the cognate resistance gene *RPS2*. In fact, RIN4 is not required for the virulence function of AvrRpt2 and AvrRpm1 (29) and leaf chlorosis caused by AvrB overexpression (41). It is suggested that other proteins associated with RIN4 might be required for the AvrRpt2 and AvrRpm1 virulence functions (29).

It is likely that RAR1 is targeted by AvrB to suppress PTI. Although the yeast two-hybrid experiments failed to detect an interaction of RAR1 with AvrB, coimmunoprecipitation detected an AvrB–RAR1 interaction. Perhaps the interaction is indirect or stabilized by a plant-specific protein. The interaction does not appear to involve RIN4, because we were not able to detect an interaction between RIN4 and RAR1. Nonetheless, it is significant that both RAR1 and RIN4 negatively regulate PTI and are targeted, directly or indirectly, by AvrB. Therefore, host proteins that negatively regulate PTI may be an Achilles' heel in innate immunity that is actively exploited by bacterial effectors. That RIN4 and RAR1 are required for the function of multiple resistance proteins suggests that these negative regulators of PTI are common "guardees" of resistance proteins (SI Fig. 13). It is possible that resistance proteins are recruited to a protein complex containing negative regulators of the PAMP signaling pathway such as RIN4 and RAR1 to monitor effectors that suppress PTI. This enables the rapid activation of effector-triggered defenses when PAMP-triggered resistance is inhibited by the virulence factors.

Materials and Methods

Mutagenesis, Mutant Screening, and Map-Based Cloning. Seeds of a homozygous *RAP2.6-LUC* transgenic line (19) were mutagenized with 0.3% (wt/vol) EMS (Sigma–Aldrich, St. Louis, MO) for 8 h and grown to maturity in 30 plant pools, and M_2 seeds were harvested. A total of 300 pools of M_2 seeds representing 9,000 M_2 families were obtained. Approximately 16,000 M_2 plants derived from all of the 300 pools were individually infiltrated with 2×10^6 cfu/ml DC3000 (*avrB*) bacteria, and inoculated leaves were removed 6 h later for the reporter assay (19). Plants with reduced LUC activity were identified as putative mutants and confirmed in the M3 generation. All experiments involving *rrb3* were carried out with a back-crossed line.

For mapping the *rrb3* gene, the *rrb3* mutant was crossed with the Nossen ecotype, and 5-week-old F_2 plants were inoculated with DC3000 (*avrB*) at 10^8 cfu/ml. Plants displaying delayed HR were scored as mutants. Simple sequence-length polymorphism (SSLP), insertion/deletion (InDel), and in-house-developed cleared amplified polymorphic sequence (CAPS) or SNP markers were used in fine mapping as described previously (42).

CCD Imaging and Luciferase Activity Assay. Four- to 6-week-old plants were infiltrated with 2×10^6 cfu/ml DC3000 (*avrB*) containing 0.02 mM luciferin. The inoculated leaves were then collected at different time points and sprayed with 1 mM luciferin containing 0.01% Triton X-100. The leaves were kept in the dark for 6 min before luminescence images were captured. Quantitative LUC assay was performed as described (19).

Production of *AvrB* Transgenic Plants. A FLAG-tagged version of *AvrB* was PCR amplified from pCPP2306 (23) by using the following primers: 5′-cgggatccccatgggctgcgtctcgtcaaaaagcac-3′ and 5′-gctctagatcacttgtcatcgtcgtccttgtag-3′. The *AvrB* fragment was ligated into pTA7002 (25) that had been digested with XhoI and then blunt ended. A resulting clone containing *AvrB* under the control of the pTA70002 Dex-inducible promoter was transformed into *Arabidopsis thaliana* Nd-0 plants (*rpm1-null*; ref. 33), as described (43). Seven independent *AvrB* transformants were analyzed, and all exhibited characteristics similar to the results reported here.

Western Blot Analysis. Anti-RAR1 antiserum was raised in rabbits by using full-length recombinant RAR1 protein as antigen as described (36). Anti-AvrB antibodies were a gift from Alan Collmer (Cornell University, Ithaca, NY). Total protein was extracted from 5-week-old plants in a 1× PBS buffer containing 10 mg/ml leupeptin, 1 mM PMSF, 2 mM EDTA, 1× proteinase inhibitor mixture (Roche, Basel, Switzerland), and 1% Triton X-100. For AvrB protein detection, plants were sprayed with 30 μM Dex (Sigma) for 24 h before protein extraction. Thirty-microgram protein samples were electrophoresed through a 12% or 15% SDS/PAGE. Protein was electrotransferred to an Immobilon P membrane (Millipore, Bedford, MA). Immunodetection was performed with a 1:2,500 dilution of anti-RAR1 antibodies or a 1:10,000 dilution of anti-AvrB antibodies. The blot was then hybridized with a goat anti-rabbit or goat anti-mouse HRP-conjugated secondary antibody (Sigma) and visualized with ECL Western blotting detection reagents (Amersham, Piscataway, NJ), following the manufacturer's instructions.

Construction of *rar1–29/rar1–29,rpm1/rpm1,AvrB/AvrB; rar1–20/rar1–20,rpm1/rpm1,AvrB/±* and *coi1/coi1,rpm1/rpm1,AvrB/±* Plants. To construct *rar1–29/rar1–29,rpm1/rpm1,AvrB/AvrB* and *RAR1/RAR1,rpm1/rpm1,AvrB/AvrB* plants, the Nd (*AvrB*) transgenic line 1 was crossed with the *rar1–29* plants (Col-0 background). The SSLP marker K17N15–19K (primers 5′-gactagagagtaagaacatgactc-3′ and 5′-aagtcgaatcgttcacgcaataag-3′) closely linked to the *RAR1* locus was used to identify the respective genotypes at the *RAR1* locus. Homozygous F_4 plants were used for experiments. *rar1–20* (21) and *coi1–1* (20) mutants (Col-0 background) were similarly crossed with Nd(*AvrB*). *rar1–20/rar1–20,rpm1/rpm1,AvrB/±* and *RAR1/±,rpm1/rpm1,AvrB/±* plants and *COI1/COI1,rpm1/rpm1,AvrB/±* and *coi1–1/coi1–1,rpm1/rpm1,AvrB/±* plants were identified from F_2 plants by PCR. The genotype at the *COI1* locus was identified by using a CAPS maker as described (20). Primers 5′-atcttcaagtctcaaagtgtgc-3′ and 5′-gattccacaagataacttgaagc-3′ were used to determine the genotype at the *RPM1* locus (Nd lacks *RPM1*). Plants carrying the *AvrB* transgene were confirmed with *AvrB*-specific primers 5′-

atcaatgcttaattggtgcagc-3′ and 5′-atcagaatctagcaagcttctg-3′. All of the plants carry a chromosome segment from the Nd ecotype and thus are *rpm1*-null.

Bacterial Growth Assay. Five-week-old plants were sprayed daily with a 30 μM Dex solution containing 0.02% Silwet L-77 (Osi Specialties, Friendship, WV). DC3000 *hrpL* mutant (26) bacterial suspension was infiltrated at 10^5 cfu/ml into leaves 2 days after the first Dex treatment. Leaf bacterial number was counted at the indicated time points. Each data point consisted of at least six replicates.

Callose Staining. To visualize callose deposition, 5-week-old *Arabidopsis* leaves were untreated or pretreated by spraying 50 μM Dex or distilled water 24 h before infiltration of flg22 at the indicated concentrations. Whole leaves were harvested at the indicated times, cleared, stained with aniline blue (27), and mounted in 50% glycerol, and fluorescence from callose was visualized with an epifluorescence microscope under UV light. For each treatment, four leaves were examined, and one microscopic field per leaf that best represented the overall staining of the leaf was used to calculate the number of callose deposits per field of 0.1 mm^2 with Image J software (www.uhnresearch.ca/wcif/imagej).

Coimmunoprecipitation. Coimmunoprecipitation experiment was done as described (12). AvrB-3xFLAG transgenic and nontransgenic *rpm1* plants (33) were sprayed with 30 μM estradiol (Sigma) before protein extraction. The immune complex was precipitated with an agarose-conjugated monoclonal anti-FLAG antibody (Sigma). The presence of RAR1 and AvrB-FLAG in the complex was detected by using Western blotting.

Yeast Two-Hybrid Assay. The *RAR1, rar1–29, SGT1b*, and *HSP90.1* coding sequences were amplified from total cDNA of *Arabidopsis* Col-0 wild-type (*RAR1*, *SGT1b*, and *HSP90.*1) or *rar1–29* plants by using gene specific primers 5′-aactctgaattcatggaagtaggatctgca-3′ and 5′-aatctcgagctttgaatcgaaaatctcagg-3′ (*RAR1* and *rar1–29*), 5′-gaattccctctgaaagaatcaatgg-3′ and 5′-ctcgagagatcaatactcccacttc-3′ (*SGT1b*), and 5′-gaattcctaaagttcgttgcgatgg-3′ and 5′-ctcgagcttcatctcttagtcgac-3′ (*HSP90.1*). PCR products were digested with EcoRI and XhoI and inserted into pJG4–5 (*RAR1* and *rar1–29*) or pEG202 (*SGT1b* and *HSP90.1*). The constructs were sequence-verified and cotransformed in pairs into the EGY48 yeast strain containing pSH18–34. At least six individual colonies from each transformation were tested for β-galactosidase activities on X-Gal plates following the protocol described (44).

To determine whether the RAR1 and rar1–29 proteins accumulated to similar levels in yeast, total yeast protein was extracted by boiling equal amounts of yeast cells in 2× Laemmli sample buffer. The total protein was separated by 10% SDS/PAGE gel and transferred to immobilon membrane (Millipore). The membrane was then hybridized with monoclonal mouse anti-HA antibody (Sigma) and detected with the HRP-conjugated goat anti-mouse antibodies (Sigma) and ECL regents (Amersham, Piscataway, NJ).

We thank Alan Collmer for anti-AvrB antibodies, Xing Wang Deng (Yale University, New Haven, CT) and Yan Guo (National Institute of Biological Sciences, Beijing, China) for plasmids, Frank White and ShengYang He for critical reading of the manuscript, and Liqin Fu for technical assistance with microscopy. J.-M.Z. was supported by a grant from the Chinese Ministry of Science and Technology (2003-AA210080). R.T. and J.Z.-V. were supported in part by a U.S. Department of Energy grant awarded to Sheng Yang He (DE-FG02–91ER20021).

1. Ausubel FM (2005) *Nat Immunol* 6:973–979.
2. Alfano JR, Collmer A (2004) *Annu Rev Phytopathol* 42:385–414.
3. Abramovitch RB, Anderson JC, Martin GB (2006) *Nat Rev Mol Cell Biol* 7:601–611.
4. Chisholm ST, Coaker G, Day B, Staskawicz BJ (2006) *Cell* 124:803–814.
5. Dangl JL, Jones JDG (2001) *Nature* 411:826–833.
6. Takahashi A, Casais AC, Ichimura K, Shirasu K (2003) *Proc Natl Acad Sci USA* 100:11777–11782.
7. Hubert DA, Tornero P, Belkhadir Y, Krishna P, Takahashi A, Shirasu K, Dangl JL (2003) *EMBO J* 22:5679–5689.
8. Lu R, Malcuit I, Moffett P, Ruiz T, Peart J, Wu A-J, Rathjen JP, Bendahmane A, Day D, Baulcombe DC (2003) *EMBO J* 22:5690–5699.
9. Bieri S, Mauch S, Shen QH, Peart J, Devoto A, Casais C, Ceron F, Schulze S, Steinbiss HH, Shirasu K, Schulze-Lefert P (2004) *Plant Cell* 16:3480–3495.
10. Holt BF, III, Belkhadir Y, Dangl JL (2005) *Science* 309:929–932.
11. Azevedo C, Betsuyaku S, Peart J, Takahashi A, Noel L, Sadanandom A, Casais C, Parker J, Shirasu K (2006) *EMBO J* 25:2007–2016.
12. Mackey D, Holt BF, Wiig A, Dangl JL (2002) *Cell* 108:743–754.
13. Axtell MJ, Staskawicz BJ (2003) *Cell* 112:369–377.
14. Mackey D, Belkhadir Y, Alonso JM, Ecker JR, Dangl JL (2003) *Cell* 112:379–389.
15. Shao F, Golstein C, Ade J, Stoutemyer M, Dixon JE, Innes RW (2003) *Science* 301:1230–1233.
16. Day B, Dahlbeck D, Huang J, Chisholm ST, Li D, Staskawicz BJ (2005) *Plant Cell* 17:1292–1305.
17. Ong LE, Innes RW (2006) *Mol Microbiol* 60:951–962.
18. Lee CC, Wood MD, Ng K, Andersen CB, Liu Y, Luginbuhl P, Spraggon G, Katagiri F (2004) *Structure (Cambridge, UK)* 12:487–494.
19. He P, Chintamanani S, Chen Z, Zhu L, Kunkel BN, Alfano JR, Tang X, Zhou JM (2004) *Plant J* 37:589–602.
20. Xie D, Feys BF, James S, Nieto-Rostro M, Turner JG (1998) *Science* 280:1091–1094.
21. Tornero P, Merritt P, Sadanandom A, Shirasu K, Innes RW, Dangl JL (2002) *Plant Cell* 14:1005–1015.
22. Ashfield T, Keen NT, Buzzell RI, Innes RW (1995) *Genetics* 14:1597–1604.
23. Gopalan S, Bauer DW, Alfano JR, Loniello AO, He SY, Collmer A (1996) *Plant Cell* 8:1095–1105.
24. Nimchuk Z, Marois E, Kjemtrup S, Leister RT, Katagiri F, Dangl JL (2000) *Cell* 101:353–363.
25. Aoyama T, Chua NH (1997) *Plant J* 11:605–612.
26. Boch J, Joardar V, Gao L, Robertson TL, Lim M, Kunkel BN (2002) *Mol Microbiol* 44:73–88.
27. Hauck P, Thilmony R, He SY (2003) *Proc Natl Acad Sci USA* 100:8577–8582.
28. DebRoy S, Thilmony R, Kwack YB, Nomura K, He SY (2004) *Proc Natl Acad Sci USA* 101:9927–9932.
29. Kim MG, da Cunha L, McFall AJ, Belkhadir Y, DebRoy S, Dangl JL, Mackey D (2005) *Cell* 121:749–759.
30. Li X, Lin H, Zhang W, Zou Y, Zhang J, Tang X, Zhou JM (2005) *Proc Natl Acad Sci USA* 102:12990–12995.
31. Gomez-Gomez L, Felix G, Boller T (1999) *Plant J* 18:277–284.
32. Zuo J, Niu QW, Chua NH (2000) *Plant J* 24:265–273.
33. Grant MR, McDowell JM, Sharpe AG, de Torres ZM, Lydiate D, J. & Dangl JL (1998) *Proc Natl Acad Sci USA* 95:15843–15848.
34. Shirasu K, Lahaye T, Tan MW, Zhou F, Azevedo C, Schulze-Lefert P (1999) *Cell* 99:355–366.
35. Austin MJ, Muskett P, Kahn K, Feys BJ, Jones JD, Parker JE (2002) *Science* 295:2077–2080.
36. Azevedo C, Sadanandom A, Kitagawa K, Freialdenhoven A, Shirasu K, Schulze-Lefert P (2002) *Science* 295:2077–2080.
37. Muskett PR, Kahn K, Austin MJ, Moisan LJ, Sadanandom A, Shirasu K, Jones JD, Parker JE (2002) *Plant Cell* 14:979–992.
38. Peart JR, Lu R, Sadanandom A, Malcuit I, Moffett P, Brice DC, Schauser L, Jaggard DA, Xiao S, Coleman MJ, *et al.* (2002) *Proc Natl Acad Sci USA* 99:10865–10869.
39. Tör M, Gordon P, Cuzick A, Eulgem T, Sinapidou E, Mert-Turk F, Can C, Dangl JL, Holub EB (2002) *Plant Cell* 14:993–1003.
40. Lorenzo O, Solano R (2005) *Curr Opin Plant Biol* 8:532–540.
41. Belkhadir Y, Nimchuk Z, Hubert DA, Mackey D, Dangl JL (2004) *Plant Cell* 16:2822–2835.
42. Xiao F, Goodwin SM, Xiao Y, Sun Z, Baker D, Tang X, Jenks MA, Zhou JM (2004) *EMBO J* 23:2903–2913.
43. Clough SJ, Bent AF (1998) *Plant J* 16:735–743.
44. Golemis EA, Serebriiskii I, Gyuris J, Brent R (1997) in *Current Protocols in Molecular Biology*, eds Ausubel FM, Brent R, Kingston RE, Moore DD, Seidman JG, Smith JA, Struhl K (Greene/Wiley, New York), pp 20.1.1–20.1.35.